Pergamon

Biorheology, Vol. 34, No. 6, pp. 443–470, 1997

0006-355X/97 $17.00 + .00

PII S0006-355X(98)00026-2

REVIEW

ULTRASOUND BACKSCATTERING FROM NON-AGGREGATING AND AGGREGATING ERYTHROCYTES–A REVIEW

GUY CLOUTIER AND ZHAO QIN

Laboratory of Biomedical Engineering, Institut de recherches cliniques de Montréal and Department of Medicine, University of Montreal, Montreal, Québec, CANADA

Reprint requests to: Dr. Guy Cloutier, Laboratory of Biomedical Engineering, Institut de recherches cliniques de Montréal, 110 avenue des Pins Ouest, Montréal, QC, H2W 1R7, Fax: 514-987-5705; e-mail: cloutig@ircm.umontreal.ca

ABSTRACT **The objective of the present paper is to provide a detailed review of theoretical, experimental and clinical works aimed at understanding the scattering of ultrasound by red blood cells (RBC). The paper focuses on the role of biofluid mechanics and blood biorheology on the scattering mechanisms. The influence of RBC aggregation on the ultrasound backscattered power is specifically addressed. After a short introduction, the paper presents the theory of Rayleigh scattering and summarizes theoretical models on ultrasound backscattering by RBC. The particle, continuum and hybrid models are presented along with reported packing factors used to consider the orderliness in the spatial arrangement of RBC. Computer models of ultrasound backscattering by RBC are also presented in this section. In the second section, experimental factors affecting the ultrasound backscattered power from blood are presented. The influence of the volume of the scatterers, ultrasound frequency, hematocrit, orientation of the scatterers, flow turbulence, flow pulsatility, and concentration of fibrinogen and dextran is discussed. The third section focuses on the use of ultrasound to characterize RBC aggregation. Three aspects are reported: the shear rate dependence of the backscattered power, the "black hole" phenomenon, and the kinetics of RBC rouleau formation. The fourth section reports *in vivo* observations of the "smoke like" echo in mitral valve disease, and blood echogenicity and backscattered power in veins and arteries. In the last section, new areas of research, clinical applications of ultrasound backscattering, and areas of potential future developments are presented.** © 1998 Elsevier Science Ltd

KEYWORDS: **Acoustic backscattering; blood echogenicity; spontaneous echo contrast; red blood cell aggregation; turbulence; power Doppler ultrasound**

Introduction

Ultrasound imaging became accepted as a diagnostic imaging modality in the early 1970s when gray-scale ultrasonography was introduced. The ultrasonic scattering properties of blood has always been of considerable interest. However, because ultrasound at diagnostic frequencies between 2 and 30 MHz cannot resolve individual blood elements, the speckle pattern occasionally seen on gray-scale B-mode ultrasound images is complex and cannot be directly related to the spatial arrangement and structure of moving RBC. Currently, we know that the fluctuation in the spatial and temporal distribution of RBC and the presence of RBC aggregation strongly contribute to the intensity of the ultrasound scattered signal. Since the early work by Reid and collaborators on ultrasound scattering by blood (Shung and Thieme, 1993), much progress has been made in this field of research. However, there is still much to learn as new discoveries often raise more questions than they answer.

Of all the techniques proposed in the literature to study the rheological properties of blood, most involve blood sampling and *in vitro* measurements (Stoltz and Donner, 1991). Ultrasound, which propagates through soft tissues, has the potential to be applied *in vivo*. Within the field of clinical hemorheology and biorheology, ultrasound has the potential to provide new insight into the understanding of the dynamics of RBC aggregation, platelet aggregation, and blood flow turbulence. This review focuses on the rheology of both nonaggregating and aggregating erythrocytes as assessed by ultrasound backscattering.

Ultrasound backscattered power from blood

RBC as scattering targets

When an acoustic wave propagates through inhomogeneous media, such as biological tissues, it is diverted by reflection and refraction from tissue interfaces, by scattering if the size of the interfering particles is much smaller than the ultrasound wavelength, or it is absorbed by the medium and converted into heat. Backscattering of ultrasound by blood is almost entirely due to the biconcave shaped erythrocytes because they are much more numerous than the slightly larger leukocytes, and significantly larger and more numerous than platelets. Typical human RBC have a diameter of approximately 8.2 μm and are roughly 2.2 μm thick.

The behavior of erythrocytes as scattering targets depends on their size, concentration, and acoustic properties. In most clinical instruments, the ultrasound frequency is in the range of 2–30 MHz. The wavelengths corresponding to these frequencies are larger than the size of a RBC (770 μm at 2 MHz and 51 μm at 30 MHz). When an incident ultrasound beam is scattered by RBC, the scattered power can be measured at any scattering angle ϕ between 0 and 360° (Shung *et al.*, 1977). Scattering measurements are made with one transducer for backscattering at 180° or by two transducers for other angular measurements.

The most widely used approach in medical ultrasound is the pulse-echo B-mode scanning technique. Using a wideband emitting pulse and recording the time variation of the radio-frequency (RF) echo envelope, gray-scale ultrasonic images are generated from the specularly reflected echoes (reflection from large interfaces) as well as from the diffusely backscattered echoes (scattering from small particles). The term *echogenicity*, specific to B-mode imaging, is used as a measure of the tissue backscattering properties, whereas the term *echoicity* is used to take into consideration the influence of both the ultrasound system and intervening tissues (Yuan and Shung, 1989). Ultrasound

received from moving scatterers has a different frequency from that of the transmitted ultrasonic signal. This change in frequency is known as the *Doppler effect* and its magnitude as the *Doppler frequency shift* which is proportional to the axial velocity of scatterers (Evans *et al.*, 1989). Due to this unique property of the Doppler effect, the Doppler technique is mainly used for the detection and measurement of blood flow velocity. The square of the intensity of the Doppler ultrasound signal backscattered by RBC is known as the *Doppler backscattered power. Power Doppler ultrasound* is a new imaging modality available on commercial instruments that maps the backscattered power in real time within vessels.

Rayleigh scattering

Theoretical models of ultrasound scattering by blood are used to understand the physical mechanisms generating the scattered signal from RBC. The backscattering coefficient (*BSC*), defined as the power backscattered by a unit volume of scatterers per unit incident intensity per unit solid angle in the backward direction (Shung and Thieme, 1993), is commonly used to characterize ultrasound scattering by blood and tissues. When an ultrasonic wave encounters a particle that is very small in size compared to the incident wavelength λ, a part of the incident energy is uniformly scattered in all directions. This kind of wave scattering was first studied by Lord Rayleigh in 1871 and is therefore referred to as *Rayleigh scattering* (Rayleigh, 1945).

The scattering cross-sectional area of a RBC is a very important parameter used to define the ultrasound backscattering properties of blood (Shung and Thieme, 1993). It is defined as the power scattered by one spherical particle per unit incident intensity per unit solid angle in a direction ϕ with respect to the ultrasound beam. By assuming Rayleigh scattering, a spherically shaped RBC, and an observation point many wavelengths distant from the scatterer,

$$(1) \qquad \sigma(\phi) = \frac{V_c^2 \pi^2}{\lambda^4}\left[\frac{k_c - k_p}{k_p} + \frac{\rho_c - \rho_p}{\rho_c}\cos\phi\right]^2$$

where $\sigma(\phi)$ is the scattering cross-sectional area (in cm^2 or any other area units) of a single RBC of radius a, $V_c = (4/3)\pi a^3$ is the volume of the scatterer, and λ is the wavelength. Parameters k_c, ρ_c and k_p, ρ_p are, respectively, the compressibility and mass density of the scatterers (RBC, subscript c) and of the surrounding medium (plasma, subscript p), and ϕ is the angular direction of the scattered signal relative to the direction of the transmitted beam. Based on Eq. *(1)*, Rayleigh scattering predicts that the backscattered power from one particle is proportional to the square of the particle volume and the fourth power of frequency ($f = c_b/\lambda$, where $c_b = 1570$ m/s is the speed of sound in blood). In practice, backscattered power measurements cannot be performed on a single particle. As discussed next, the interaction between RBC and their spatial and temporal arrangements also affect the backscattered power.

Modeling of ultrasound backscattering by RBC

For human blood at a normal hematocrit ($\approx 45\%$), the RBC are densely packed, the positions of any pair of scatterers being neither uncorrelated nor perfectly correlated in space and time. Indeed, the RBC interact strongly and cannot be treated as independent scatterers. In order to develop stochastic models for the study of the ultrasound backscattered power by RBC, different approaches were proposed. Two basic classical approaches are known as the particle and continuum methods. These two methods are basically different

ways of modeling the density and compressibility functions of the random medium, which lead to an inhomogeneous wave equation with different source terms. The source terms in the particle model are the backscattered wavelets from individual RBC, while those in the continuum model are the density and compressibility fluctuations of the medium generating the scattered signal. In both models, because scattering from RBC is very weak, multiple scattering is generally ignored. Alternative approaches of modeling ultrasound scattering by RBC can be found in Hanss and Boynard (1979) and Cobet (1988). The following subsections summarize the particle and continuum approaches reviewed in detail by Mo and Cobbold in Chapter 5 of Shung and Thieme (1993).

The particle model

Brody and Meindl (1974) and Albright and Harris (1975) were the first to develop particle models for ultrasound scattering. They assumed RBC to be independent point-sized particles. Shung *et al.* (1976) adapted a heuristic "hole" approach to explain backscattering by RBC in their model. Mo and Cobbold (1986) proposed a more general particle scattering model assuming blood as a suspension of RBC aggregates, all much smaller than the wavelength. With H as the hematocrit, V_c as the volume of the scatterers, W as the packing factor which is a measure of the correlation amongst scatterers ($W = 1$ for completely random placement and $W \to 0$ as the placement becomes ordered), and assuming that all scatterers in the insonificated blood sample are identical in size, the *BSC* is given by:

$$BSC = \sigma_{bs} (H / V_c) W \qquad (2)$$

where σ_{bs} is the backscattering cross-section obtained from Eq. *(1)* for $\phi = 180°$. At very low hematocrits, W is equal to unity so that the *BSC* is simply proportional to H. As the hematocrit is increased, W decays gradually to zero since closer packing will invariably lead to a greater orderliness in the scatterer spatial arrangement. From Eqs. *(1)* and *(2)*, it can be seen that at a given hematocrit *BSC* is proportional to the volume of the scatterers weighted by the packing factor and to the fourth power of the frequency.

The continuum model

In the continuum model, it was suggested that due to the limited resolution of the ultrasound beam, RBC and small RBC aggregates cannot be individually recognized, because they are much smaller than the wavelength. With this model, scattering is considered to arise from spatial fluctuations in the density and compressibility of the continuum. By adapting the equations proposed by Angelsen (1980), Mo and Cobbold (see Chapter 5 of Shung and Thieme, 1993) proposed the following expression for the backscattering coefficient:

$$BSC = \frac{\pi^2}{\lambda_m^4}\left[\frac{k_c - k_p}{k_m} - \frac{\rho_c - \rho_p}{\rho_m}\right]^2 V_c^2 (1/\Omega_e)\overline{\mathrm{var}(n)} \qquad (3)$$

where the subscript m means the average of the corresponding parameter in the random medium, Ω_e is the elemental blood volume considered, also known as a voxel, and $\overline{\mathrm{var}(n)}$ is the variance in the number of scatterers in Ω_e obtained by averaging over space and time. In Eq. *(3)*, λ_m is the average wavelength in the random medium which varies with the hematocrit. In Angelsen's approach, the motion of RBC is allowed and the effects of the transfer function of the Doppler receiver and that of the transducer can be taken into account. An

alternative approach based on Chernov's equations and statistical mechanic theories was proposed to model blood as a continuum (Shung and Kuo, 1994). In that model, the backscattering coefficient as a function of the hematocrit for nonaggregating RBC matched well simulated results obtained with the particle approach.

The hybrid model

To generalize both particle and continuum approaches, the hybrid model was suggested (Mo and Cobbold, 1992). In this model, the RBC within a voxel Ω_e are treated as a single scattering unit moving at a single velocity. The backscattering coefficient is obtained by first determining the contribution from a single scattering unit as in the particle model, with the exception that the basic scattering unit is now a voxel containing many RBC. Secondly, the contribution from all the voxels is summed by considering the influence of the mean number of scatterers per voxel and its variation in number as a function of time. Based on this approach, the *BSC* is given by:

$$(4) \qquad BSC = \frac{\sigma_{bs}\overline{\mathrm{var}(n)}}{\Omega_e}$$

or equivalently by

$$(5) \qquad BSC = \sigma_{bs}(\bar{n}/\Omega_e)W \quad ,$$

where $\bar{n}$ is the mean number of scatterers in the voxels Ω_e and W is the packing factor.

The packing factor

Based on the prior work by Twersky, Shung (1982) proposed a packing factor for blood expressed in terms of H as follows:

$$(6) \qquad W = \frac{(1-H)^4}{(1+2H)^2} \quad .$$

This packing factor explains the nonlinear relationship between ultrasound backscattering and high values of hematocrit. Very recently, a new theoretical model that used a fractional packing dimension to represent the manner in which the RBC are packed was proposed (Bascom and Cobbold, 1995). In this model, the packing factor is given by:

$$(7) \qquad W(m) = \frac{(1-H)^{m+1}}{(1+H[m-1])^{m-1}} \quad ,$$

where m is the fractional packing dimension related to the physical dimension and the packing symmetry of the scatterers. According to this model, m is related to the absolute temperature, the Boltzmann's constant, the pressure within the fluid, the variation with respect to the pressure of the isothermal compressibility of the fluid, and the flow conditions. For $m = 3$ (spherical packing), Eq. *(7)* is equivalent to Eq. *(6)*. By fitting this model to experimental results, it was shown by Bascom and Cobbold (1995) that $m = 2.54$ for porcine RBC suspended in a saline solution (no aggregation) under steady laminar flow. Substituting Eq. *(6)* or *(7)* into Eq. *(5)* yields the *BSC* for blood.

Using the theory of scaled particle statistical mechanics, Twersky (1988) obtained a packing factor based on the fluctuation characteristics of the particle number in a sample volume for mixtures of similar-shaped but different-sized scatterers. He introduced two parameters in his model: parameter c that considers the shape and correlation among particles, and parameter d that represents the variance of the particle size. According to this model, the packing factor is given by:

$$(8) \qquad W(c,d)=\frac{(1-H)^2}{\left[1+(c-1)H\right]^2}\left[(1-H)^2+\frac{4cdH(1-H)}{1+5d}+\frac{H^2c^2d}{1+4d}\right] .$$

Different values of parameters c and d were obtained for bovine and human red cells suspended in a saline solution under different flow conditions (Berger *et al.*, 1991). To date, no data obtained under RBC aggregation conditions were fitted to the models of Eqs. *(6)* to *(8)*.

Computer models of ultrasound backscattering by RBC

A one-dimensional computer simulation model of continuous-wave ultrasound scattering by RBC was proposed by Routh *et al.* (1987). In that model, the RBC were represented by rows of identical, finite-sized elements separated by randomly sized sections representing the plasma. By changing the mean distance between rows of scatterers, the backscattered power as a function of the hematocrit could be studied. The effect of increasing the number of scatterers and the influence of the insonating frequency were evaluated. The simulations showed some agreement with the experimental results. The model also indicated a large variance in the backscattered power, which is analogous to what is observed experimentally with blood. In this simulation, the phenomenon of RBC aggregation was considered negligible.

Following that study, the model was improved by considering a chain that was fixed at both ends and contained n slabs (Gough *et al.*, 1988) and a chain of randomly spaced identical slabs (Routh *et al.*, 1989). Both one-dimensional approaches were used to model the backscattered power as a function of the hematocrit and the results predicted the maximum backscattered power at around 35% hematocrit. In the simulation, a second peak at approximately 90% hematocrit was found (Routh *et al.*, 1987; 1989). By using randomized boundary conditions instead of fixed boundaries in the last model, Mo *et al.* (1994) showed that the second peak was artifactual. Based on current knowledge, the predicted peak at 35% hematocrit for this one-dimensional model disagrees with experimental observations, as discussed in the next paragraph.

The scattering of ultrasound as a function of the hematocrit and scatterer size was further studied using one- and two-dimensional computer simulation models (Zhang *et al.*, 1994). In two dimensions, scatterers were randomly positioned one by one and they were represented as a group of parallel infinitely long cylinders embedded in a homogeneous medium. In one dimension, the maximum backscattered power also occurred at around 35% hematocrit. In two dimensions, the power peaked at around 22% hematocrit, which is closer to that observed experimentally. It is expected that a computer model that would consider the three-dimensional spatial arrangement of scatterers would provide better results. Lastly, the following two computer models proposed to predict scattering from tissues are herewith reported because they may be useful for studying scattering by RBC. Hunt *et al.* (1995) showed in one and two dimensions that differences in the backscattered power

can be attributed to the spatial organization of scatterers. Recently, instead of considering each scatterer individually, one- and two-dimensional voxel approaches were proposed as a method to reduce the computation time of the simulation (Lim *et al.*, 1996).

Experimental factors affecting the ultrasound backscattered power from blood

It is recognized that several factors can influence the ultrasound backscattered power from blood. Experimental measurements were performed to validate the theoretical models described above, whereas other studies were aimed at improving our understanding of scattering by red cells.

The volume of the scatterers

Borders *et al.* (1978) showed that at frequencies between 5.2 and 12.6 MHz the Doppler backscattered power from nonaggregating RBC of different species was a function of the square of the RBC volume, for a constant cell concentration and a low hematocrit (< 10%). Their experimental results showed that dog blood (RBC volume = 74 μm^3) scatters approximately 17 times more energy than goat blood (RBC volume = 18 μm^3). These results are in agreement with the particle model of Eq. *(2)* for a cell concentration H/V_c = a constant and $W \approx 1$. Using a 6 MHz ultrasound transducer, Boynard and Lelièvre (1990) proposed that the backscattering coefficient may be related to the mean size of RBC aggregates induced by dextran of different molecular weights and concentrations. They suggested that the scattered ultrasonic intensity should be proportional to the square of the RBC aggregate volume. Based on the models described in the last section, this is oversimplification even when it is assumed that the aggregates are spherical and have dimensions much less than a wavelength. At best, the backscattered power can be related to the volume of the aggregates weighted by the packing factor, at a constant hematocrit. The variance in the size of the aggregates, their structure, and orientation for long rouleaux may also play a significant role on the backscattered power.

The ultrasound frequency

Yuan and Shung (1988b) showed, for bovine blood (no aggregation) under laminar flow conditions, that the ultrasound frequency dependence of the backscattered power was close to the fourth power assumed for Rayleigh scattering. Using porcine RBC suspensions, Kuo and Shung (1994) showed that this fourth power dependence was valid up to 30 MHz. However, using porcine whole blood at low shear rates, the frequency dependence was found to be smaller than the fourth power because of the presence of RBC aggregation (Yuan and Shung, 1988b). This last study suggests that Rayleigh scattering may no longer be valid for blood forming aggregates, especially when the ultrasound insonification frequency is high.

The hematocrit

Shung *et al.* (1976) and Borders *et al.* (1978) studied the relationship between the backscattered power and the hematocrit but their results contained artifacts. Later, it was shown that the backscattered power by porcine RBC suspensions under laminar flow increases with increasing hematocrits, peaks near 13% hematocrit, and decreases when the hematocrit is further increased (Yuan and Shung, 1988a). Using bovine and canine whole blood forming few or no RBC aggregates, similar results were obtained (Yuan and Shung, 1988a;

Yamada *et al.*, 1992). In the presence of flow turbulence, the peak of the backscattered power as a function of the hematocrit occurs around 20% hematocrit (Shung *et al.*, 1984). Beyond 20%, the power drops as observed under laminar flow. Figure 1 summarizes experimental results obtained by Shung *et al.*, (1992) for both types of flow conditions. At hematocrits below approximately 10%, few differences in the backscattered power are noted between laminar and turbulent flows.

Based on the *BSC* of Eqs. *(2)* and *(5)*, the nonlinear relationship of the backscattered power beyond 13% hematocrit can be explained by the packing effect of RBC. Using porcine whole blood under laminar flow conditions, the backscattered power as a function of the hematocrit is affected by the flow velocity or shear rate (Shung *et al.*, 1992). As indicated in Fig. 2, the power peaks near 13% hematocrit at a high velocity, while at a low velocity, a plateau and larger variances between experiments are observed for hematocrits higher than 13%. The larger variance can be explained by the presence of RBC aggregates of different sizes. The plateau may be associated with the opposing effect of the hematocrit on the packing factor and RBC aggregate size enhancement. As the hematocrit is increased beyond 13%, the correlation among scatterers may increase, leading to a backscattered power reduction that is compensated for by the increase of the mean aggregate size. A continuous increase up to 32% hematocrit was observed in another study with RBC suspended in dextran under stationary flow conditions (Boynard and Lelièvre, 1990).

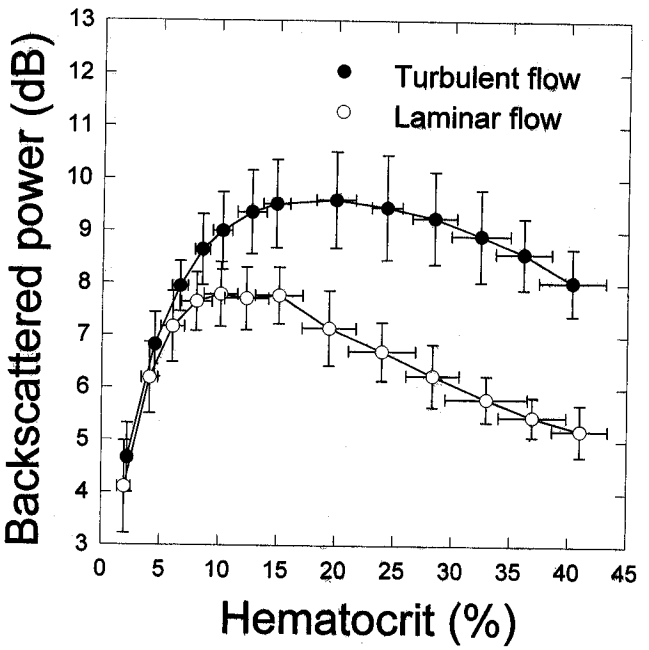

Fig. 1. Doppler power backscattered by porcine erythrocytes suspended in a saline solution as a function of the hematocrit. Experiments were repeated five times under steady laminar and turbulent flow conditions (the error bars represent the standard deviations). Doppler measurements were performed at the center of the 4.8 mm diameter tube. Turbulence was induced by introducing a screen mesh in the flow model. (Figure modified from Shung *et al.*, 1992.)

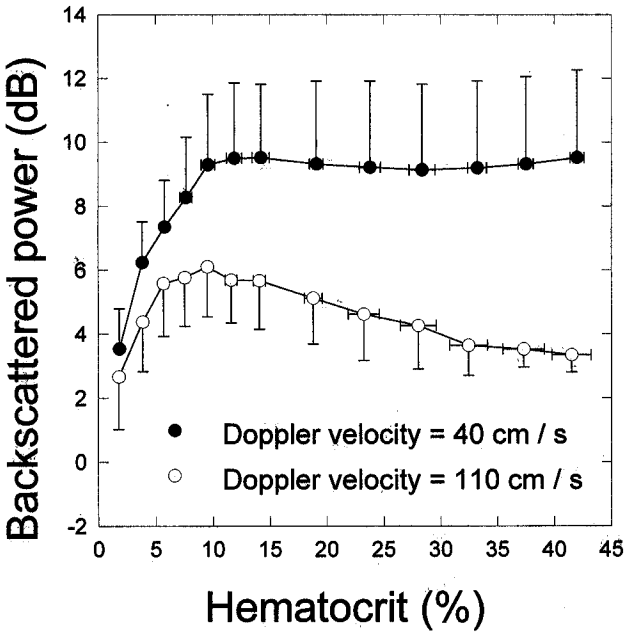

Fig. 2. Doppler power backscattered by porcine whole blood under steady laminar flow as a function of the hematocrit and Doppler velocity. The error bars represent the standard deviations computed from five experiments. Doppler measurements were performed at the center of a 4.8 mm diameter tube. (Figure modified from Shung *et al.*, 1992.)

The orientation of the scatterers

Based on Rayleigh scattering, the shape and orientation of scatterers have no effect on the backscattered power. However, in the presence of RBC aggregation and under steady laminar flow, Allard *et al.* (1996) observed an angular dependence of the backscattered power at some specific shear rate conditions for porcine whole blood. The maximum Doppler power was obtained at insonification angles between 45° and 60° with respect to the tube axis. It was suggested that among possible mechanisms to explain this anisotropic effect, the geometry of the RBC aggregates at the center of the tube may be a determining factor. In another recent study by our group (Qin *et al.*, 1998a), anisotropy of the backscattered power was also found around the center of the tube with horse blood. The anisotropy may be explained by the fact that horse blood forms long chains of RBC aggregates (Weng *et al.*, 1996).

The flow turbulence

Shung *et al.* (1984) were the first to demonstrate that flow disturbance increases the ultrasound backscattered power. Following that study, Shung *et al.* (1992), Bascom *et al.* (1993), Cloutier and Shung (1993a), Cloutier *et al.* (1995; 1996a), and Bascom *et al.* (1997) investigated the effect of turbulence on the Doppler power backscattered by non-aggregating RBC. The mapping of turbulence, based on the backscattered power, correlated well with hot-film anemometry (Cloutier *et al.*, 1996a) and photochromic flow visualization measurements (Bascom *et al.*, 1997) performed downstream of stenoses. Under pulsatile flow (Cloutier and Shung, 1993a; Cloutier *et al.*, 1995), the ultrasound backscattered

power peaked early after peak systole when turbulence is known to be maximum. The mechanism by which turbulence affects the backscattered power is not fully understood. Twersky and collaborators (Twersky, 1987; Lucas and Twersky, 1987) assumed that turbulence decreases the correlation among scatterers (parameter c of Eq. *(8)*). Mo and Cobbold (1992) suggested that turbulence increases the fluctuations in the particle concentration within elemental voxels (parameter $\overline{\text{var}(n)}$ of Eq. *(4)*). In Bascom and Cobbold (1995), turbulence reduces the packing dimension of their fractal model (parameter m of Eq. *(7)*), which is consistent with an increase in the particle concentration variance. Although different, all three studies agree on the same point: turbulence produces randomness in the spatial and temporal arrangement of RBC that leads to an increase in the backscattered power.

The pulsatility of the flow

The effect of the flow pulsatility on the ultrasound backscattered power was first reported *in vivo* by De Kroon *et al.* (1991) and *in vitro* by Cloutier and Shung (1991). Using an intravascular probe operating at 30 MHz, De Kroon *et al.* (1991) reported changes in ultrasound echogenicity during the cardiac cycle in three patients. They proposed that these variations could be related to changes in the state of RBC aggregation induced by the varying shear rate. By circulating porcine whole blood at 40% hematocrit in a flow model (Cloutier and Shung, 1993b), a significant cyclic variation of the Doppler power was also reported at 10 MHz along with a low pulse rate of 20 beats/min. However, at a pulse rate of 70 beats/min, no power variation was found within the flow cycle. It was suggested that the cyclic power variation may be due to RBC aggregate formation and disruption, and rouleau orientation.

These last results were confirmed in a recent study (Wu and Shung, 1996), in which the influence of the radial position of the sample volume within the tube and that of the tube compliance was also evaluated using a 10 MHz transducer. By moving the sample volume closer to the wall, the backscattered power peaked earlier in the flow cycle at a low pulsation rate, due to the effect of the higher shear rate on RBC aggregation. In the study of De Kroon *et al.* (1991), the presence of a cyclic variation at a physiological pulsation rate and the absence of power variations in the last two studies at 70 beats/min may be due to the different ultrasound carrier frequency selected. Because the aggregates are probably smaller at 70 beats/min, the resolution at 10 MHz may not be sufficient to observe a cyclic variation. Finally, as reported by Cloutier and Shung (1993a); Cloutier *et al.* (1995); and Bascom *et al.* (1997), flow turbulence can also induce a cyclic variation of the Doppler power at a high hematocrit. Unless the flow condition is known, the cyclic variation due to turbulence and RBC aggregation may be difficult to dissociate.

The concentration of fibrinogen and dextran

Yuan and Shung (1988b) showed that the ultrasound backscattered power from porcine whole blood under laminar flow conditions increases with rising fibrinogen concentrations due to the presence of RBC aggregation. Boynard and Lelièvre (1990) studied the ultrasound backscattered power for human blood suspended in different molecular weights and concentrations of dextran saline solutions. They showed, for different hematocrits, that the backscattering coefficient increases with increasing dextran 70 concentration, rises up to a maximum value at a mass concentration close to 40 g/l, and then decreases. The maximum values of the backscattering coefficient for dextrans 150, 500 and 2000 were approximately the same at 20% hematocrit, were obtained at a mass

concentration close to 40 g/l, and had a higher magnitude compared to dextran 70. For all molecular weights, the backscattering coefficient increased, peaked and then decreased as the mass concentration was raised.

Use of the ultrasound backscattered power to characterize erythrocyte aggregation

Although it is currently difficult to determine the exact contribution of the rouleau size, shape, number, and packing organization on ultrasound backscattering, B-mode blood echogenicity and Doppler backscattered power provide very useful information on the reversible process of RBC aggregation.

The shear rate dependence of the backscattered power

Sigel *et al.* (1982) were the first authors to show that the ultrasound echogenicity was shear rate dependent. They suggested that RBC aggregation was an important cause of the increased blood echogenicity *in vitro* (Sigel *et al.*, 1983). According to their experimental observations with an A-mode ultrasound instrument, the echogenicity of blood was related to the flow velocity and the presence of flow stasis. They proposed that scattering from individual red cells was probably the dominant cause of blood echogenicity at high shear rates. However, they suspected that scattering from RBC aggregates was important, especially at a lower shear rate. Yuan and Shung (1988a) investigated the backscattered power from bovine and porcine whole blood at different mean shear rates. The backscattered power of porcine whole blood decreased as the shear rate was increased, whereas that of bovine whole blood was found to be independent of the shear rate. It was postulated in this study that RBC aggregation was the primary mechanism responsible for these differences.

According to the work of Shehada *et al.* (1994) summarized in Fig. 3, porcine blood echogenicity at 7 MHz and 28% hematocrit is high at stasis but a very low shear rate (between 0.5 and 2 s^{-1}) can enhance the backscattered power to a maximum because of the higher kinetics of rouleau formation associated with the enhanced cell-to-cell interactions. As the shear rate is increased beyond that associated with the maximum echogenicity, the backscattered power is reduced because rouleaux of RBC are broken down by the shear forces of the flow. In a recent study by our group (Qin *et al.*, 1998a), curves similar to those reported in Fig. 3 were obtained at 10 MHz with horse blood at 40% hematocrit. However, the shear rates corresponding to the maximum power were higher and ranged between 1 and 25 s^{-1} depending on the flow rate. The higher adhesive strength between RBC for horse blood compared to porcine blood, and the structural organization of rouleaux within the tube, proposed in this study, can explain these results. Using a high frequency 30 MHz ultrasound transducer and a Couette flow arrangement, Van Der Heiden *et al.* (1995) studied the relationship between the backscattered power, the local shear rate, and RBC aggregation at a normal hematocrit. As shown in Fig. 4, no shear rate dependence was observed for human RBC suspended in a saline solution (R^-) at shear rates below 80 s^{-1}. For both human whole blood (B) and RBC suspended in a dextran 200 solution at a concentration of 4.5 g/l (R^+), similar shear rate dependencies were observed. For instance, the backscattered power was constant below 1 s^{-1} and dropped as the shear rate was increased. For shear rates in the approximate range of 80–1000 s^{-1}, the backscattered power was stronger for whole blood than dextran suspended RBC.

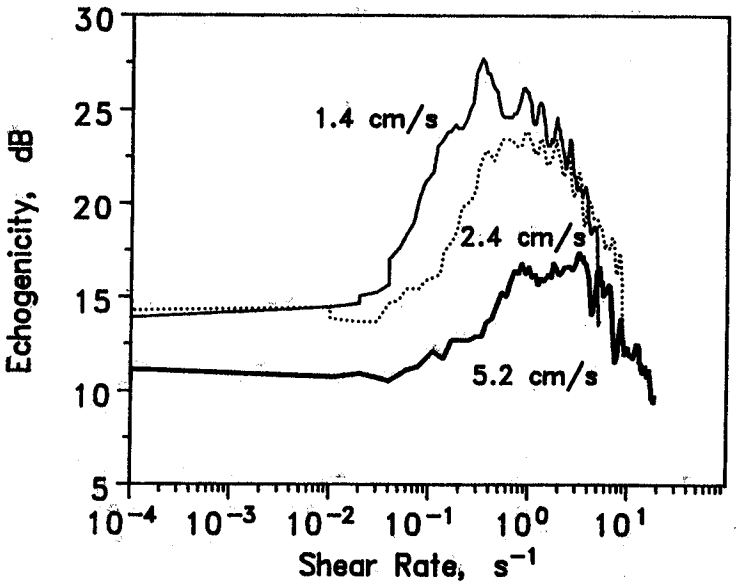

Fig. 3. Ultrasound echogenicity of porcine whole blood at 28% hematocrit as a function of the shear rate for mean velocities across the tube varying between 1.4 and 5.2 cm/s. Modal shear rate variations of the echogenicity were observed for all measurements. Experiments were conducted in a 2.54 cm diameter tube under steady laminar flow. (Reproduced from Shehada *et al.* (1994) with permission from Elsevier Science Ltd, UK.)

Recently, our group studied the shear rate dependence of porcine RBC aggregation using the Doppler ultrasound technique and a steady laminar flow model (Cloutier *et al.*, 1996b). For each flow rate tested, several measurements were performed from different radial positions across the tube. It was observed that 1) the Doppler power was usually minimum close to the wall and maximum around the center of the tube, where the local shear rate was minimum; 2) when the flow rate was varied from 1500 to 125 ml/min, the backscattered power increased by 12.4 dB; and 3) the variation of the Doppler power as a function of the shear rate within the sample volume (measured from the velocity profile and the ultrasound beam characteristics) showed three specific regions (Fig. 5). These regions corresponded to a rapid reduction of the power between 1 and 5 s^{-1} that was postulated to be associated with the disruption of large three-dimensional aggregates, a zone between 5 and 10 s^{-1} having a smaller reduction of power due to the dissociation of large rouleaux, and a region above 10 s^{-1} with a small variation of power presumably related to the separation of small rouleaux, consisting of a few RBC. In a recent study (Cloutier and Qin, 1997), the shear rate dependence of RBC aggregation was evaluated using normal, hypo-aggregating, and hyper-aggregating erythrocytes. Similar power decaying curves as a function of the local shear rate were obtained. However, the power for a given shear rate was higher for blood samples characterized by a higher kinetics of aggregation. In this study, the flow rate dependence of RBC aggregation was also evaluated using the power Doppler imaging technology.

According to Fig. 5, no aggregates, or at least none large enough to be detected at 10 MHz, are present beyond 20 s^{-1}, approximately. It is interesting

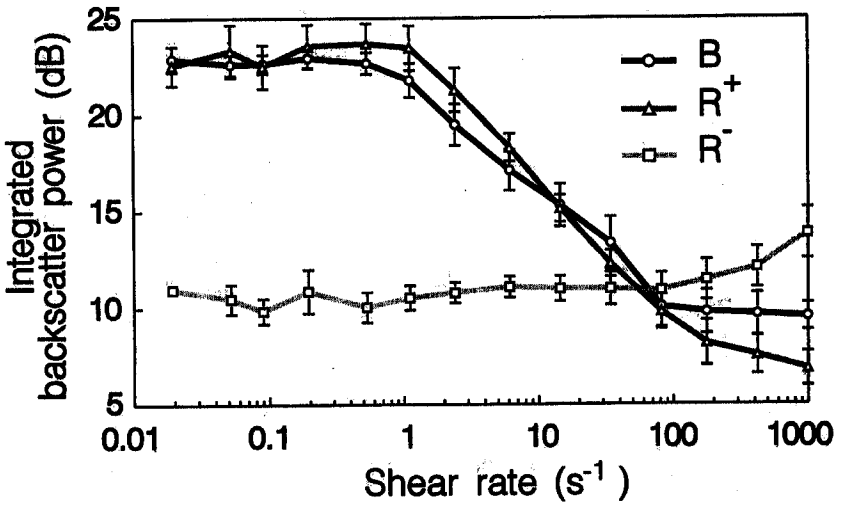

Fig. 4. Shear-rate dependence of the integrated backscattered power for human whole blood (B), human RBC suspended in a dextran 200 solution (R^+), and human RBC suspended in a 0.9% saline solution (R^-) at a normal hematocrit. The error bars represent the standard errors of the mean. (Reprinted with permission from Van Der Heiden *et al.* (1995), Elsevier Science Ltd.)

to note that these results are not in agreement with those reported in Fig. 4. For instance, in Fig. 4 the backscattered power continued to drop significantly up to 80 s^{-1} for normal human blood and up to 1000 s^{-1} for rouleau-enhanced blood. Although both figures were obtained under different flow conditions (Couette flow between coaxial cylinders for Fig. 4 and steady laminar flow in a vertical tube for Fig. 5), the discrepancies may be related to the ultrasound carrier frequency used. At 30 MHz, the backscattered power should be more sensitive to the disruption of rouleaux consisting of a few RBC. Moreover, it is possible that the backscattered power may also be influenced by the orientation of rouleaux and the deformation of RBC at that frequency. These factors should be considered in interpreting the results of Fig. 4. Besides the aforementioned studies, preliminary results on the shear rate dependence of human RBC aggregation were reported by Razavian *et al.* (1995).

The "black hole" phenomenon

By imaging porcine whole blood at 7.5 MHz under steady laminar flow in a large diameter tube, Yuan and Shung (1989) first reported the observation of a "black hole" in cross-sectional ultrasound B-mode images. These images were characterized by a hypoechoic hole near the center of the flow conduit at some shear rates and a high hematocrit (Fig. 6). The origin of the "black hole" and the mechanism responsible for its appearance were not clear at the time of study, but they were shown to be affected by the shear rate. Using a 7 MHz B-mode system, Mo *et al.* (1991) recorded images of porcine whole blood at 28% hematocrit for different entrance distances in a large diameter tube. From the images obtained at a constant mean flow velocity of 1.4 cm/s, they showed that the hypoechoic zone in the central axis of the tube appeared when increasing the inlet length of the tube. Near the entrance, the tube was almost echo free. Further downstream, the echo appeared in the periphery of the tube

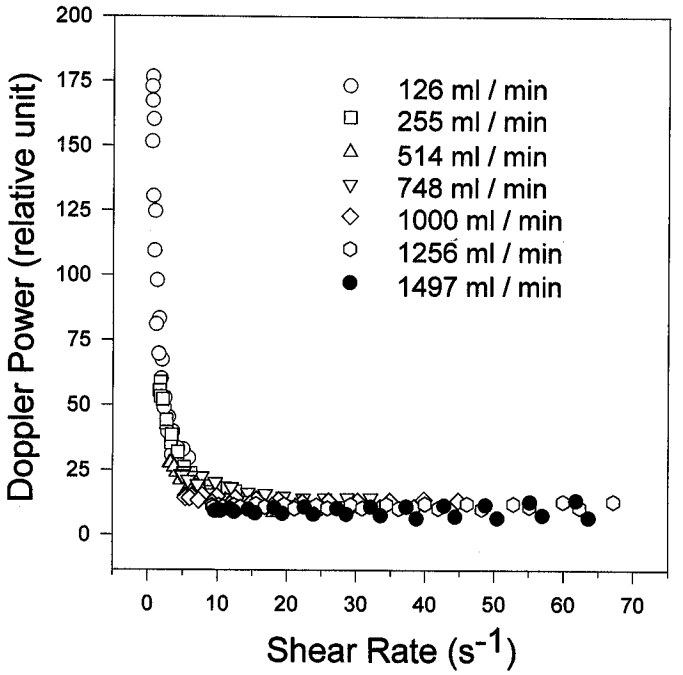

Fig. 5. Doppler power as a function of the mean shear rate within the Doppler sample volume for porcine whole blood circulated in a vertical steady flow model at 40% hematocrit. The legend gives the flow rate measured with an electromagnetic flowmeter. (Figure modified from Cloutier *et al.*, 1996b.)

and the central hypoechoic zone was developed. They suggested that the "black hole" arose from disaggregated RBC that had had insufficient time to reaggregate when they reached a steady state at the center of the tube. They also reported that suspensions of RBC in saline did not display evidence of a "black hole" when imaged, which strongly supported the hypothesis that RBC aggregation was responsible for the development of this phenomenon.

The relationship between the kinetics of RBC aggregation and the development of the "black hole" was further studied by Shehada *et al.* (1994). The blood echogenicity across the tube was measured and expressed as a function of the local shear rate obtained from the velocity profile (see Fig. 3). They observed a hypoechoic central zone with a surrounding hyperechoic ring that was dependent on the mean flow velocity. They explained the "black hole" as follows: at the entrance of the tube, the shear rate was high enough everywhere to fully disrupt all aggregates, leading to a uniform echogenicity. When the flow was fully developed, they observed a low echogenicity in the central zone of the tube attributed to shear rates lower than 0.05 s^{-1}. Blood within the region surrounding the central zone was subjected to higher shear rates favorable for the enhancement of RBC aggregation (0.05 to 2 s^{-1}, approximately), thus producing the higher echogenicity. For blood close to the wall, the shear rate was maximum but not enough to significantly disrupt RBC aggregates, thus producing a visible echo.

In a recent study by our group (Qin *et al.*, 1998a), another mechanism was shown to be involved in the "black hole" phenomenon. Using horse blood

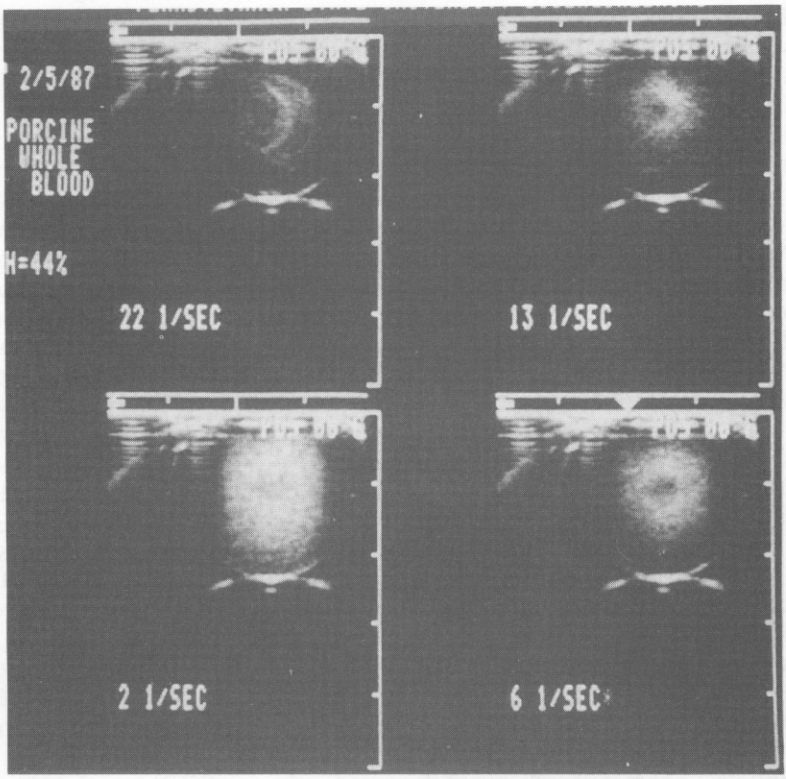

Fig. 6. The "black hole" in cross-sectional ultrasound B-mode images of porcine whole blood under steady laminar flow at varying mean shear rates and a hematocrit of 44%. The hypoechoic zone appears near the center of the flow conduit and is the most visible at a mean shear rate of 6 s^{-1}. (Figure reproduced with permission from Yuan and Shung, 1989.)

models characterized by different levels of RBC aggregation, a reduction of the Doppler backscattered power was observed at the center of the tube for steady flow rates varying between 100 and 1250 ml/min. The "black hole" was more pronounced for RBC with a high kinetics of aggregation and measurements with increasing Doppler angles. The "black hole" was observed for shear rates up to 25 s^{-1} near the center of the tube. In addition to the modal relationship of the shear rate dependence of RBC aggregation and the dynamics of rouleau formation related to the entrance distance, RBC rouleau orientation and their structural organization within the tube were suggested to play a role in the mechanism leading to the "black hole". A schematic representation of the rheological behavior of horse RBC in a large tube under steady flow was presented in that study (Qin *et al.*, 1998a).

The kinetics of RBC rouleau formation

Following a sudden flow stoppage, Shung and Reid (1979) recorded the time response of the backscattering amplitude from human blood samples at a low hematocrit (8.2%). They showed that the backscattering amplitude increases initially after stoppage and reaches a plateau in about 2–4 min. At high fibrinogen concentrations, the backscattering amplitude increases more rapidly and the final value is higher than that found at lower concentrations. Boynard

et al. (1987) also showed that the ultrasound backscattering coefficient increases with time after stopping the stirring of human blood. Their study included the phases of rouleau formation and sedimentation of RBC aggregates. Kim *et al.* (1989) showed that the buildup rate of human blood echogenicity after flow stoppage is inversely proportional to the hematocrit for hematocrits between 15 and 60%. Similar results were obtained by Kitamura *et al.* (1995) for hematocrits varying between 20 and 60%. In addition to this last observation, a plateau of the echogenicity obtained earlier at high hematocrits was shown. An explanation for these results may be that a steady-state aggregate size had already been reached before stopping the flow. Because the aggregate size corresponding to this steady-state may be proportional to the hematocrit, the buildup rate of the echogenicity was slower at high hematocrits and the plateau corresponding to the maximum aggregate size reached was attained earlier. Very recently, Sennaoui *et al.* (1997) proposed an analytical model to describe the backscattered power increase during the process of human rouleau formation. The initial phase, the rate of power increase, and the final backscattered power were studied as a function of the hematocrit and dextran concentration. The same group (Boynard *et al.*, 1994) had previously proposed a fractal model and the spectral analysis of the backscattered echoes as a method to describe the formation of spherical RBC aggregates and their sedimentation.

In all of the aforementioned studies, measurements were performed under static conditions and disaggregated RBC were expected at the beginning of the echo recording. According to Fig. 3 and previous results by Chien (1976) and Copley *et al.* (1976), keeping a very low shear rate instead of totally stopping the flow can be favorable for the enhancement of RBC aggregation. Using horse blood models, characterized by different levels of RBC aggregation, and ultrasound backscattering, our group (Qin *et al.*, 1998b) recently evaluated the influence of a complete flow stoppage and sudden flow reductions on the kinetics of rouleau formation. For all blood samples studied, no power increase was observed following flow stoppage. The flow rate (postreduction) had to be maintained low, but not totally stopped, to observe an increase in the backscattered power. The echo buildup was faster and stronger when the postreduction flow rate was increased. An unexpected pattern of variation of the backscattered power was found for horse RBC characterized by a high kinetics of rouleau formation. Instead of increasing gradually with time, the power rapidly reached a plateau and increased before reaching another plateau. Rouleau formation, random disorientation and reorientation were postulated to explain the phasic power increase observed.

In vivo characterization of erythrocyte aggregation

In addition to the *in vivo* cyclic variation of blood echogenicity mentioned earlier (De Kroon *et al.*, 1991), other studies reported "smoke like echoes", blood echogenicity variations and backscattered power differences in heart cavities, veins, and arteries. The etiology of these echoes, when identified, was generally associated with elevated levels of RBC aggregation.

The "smoke like echo" in mitral valve disease

Using M-mode echocardiography, intracardiac echoes in patients with mitral prosthetic valves were first reported in 1975 (Schuchman *et al.*, 1975). Beppu *et al.* (1985) observed a "smoke-like echo" in the left atrial cavity of patients with mitral valve disease. They suggested that these echoes were generated by flow stasis implicating RBC aggregation. The smoke-like echo vanished after

entering the left ventricular cavity and they hypothesized that this was due to the fact that the flow velocity through the narrowed mitral orifice produces disturbances which disrupt the aggregates of RBC. Today, using mainly transesophageal B-mode echocardiography, the etiology of similar echoes observed under stasis conditions in the left heart of patients with mitral valve disease and dilated cardiomyopathy is associated with RBC aggregation (Beppu *et al.*, 1985; Erbel *et al.*, 1986; Wang *et al.*, 1992; Siostrzonek *et al.*, 1993; Briley *et al.*, 1994). Some controversies existed in the literature as to whether platelet aggregates or RBC aggregates were the source of these echoes (Mahony *et al.*, 1989; 1994; Kearney and Mahony, 1995), because ultrasound can detect platelet aggregates *in vitro* (Machi *et al.*, 1984; 1987; Mahony, 1987). In a recent study (Fatkin *et al.*, 1997), spontaneous echo contrast was quantified *in vitro* using antithrombotic therapy and RBC disaggregatory agents and it was concluded that protein-mediated RBC aggregation is the mechanism of smoke-like echoes. Clinically, it was shown that intracardiac spontaneous echo contrast is a significant predictor of thrombus formation (Daniel *et al.*, 1988; Black *et al.*, 1991; Hwang *et al.*, 1994; Shen *et al.*, 1996). However, the mechanism by which RBC aggregation is implicated in thrombus formation is currently unknown.

The echogenicity and backscattered power in veins and arteries

Machi *et al.* (1983) observed greater echogenicity in the venous system when compared to the arterial system of surgically exposed vessels in dogs. They proposed that RBC aggregation enhanced by the lower shear rate in the venous system was the major source of this higher echogenicity. In humans, B-mode echoes were first seen in the inferior vena cava of a 66 year-old man suffering from constrictive pericarditis (Hjemdahl-Monsen *et al.*, 1984). In another study on 80 patients, spontaneous jugular vein echoes were observed on B-mode following carotid endarterectomy and this finding plus the early appearance of neointima were found to be predictive of restenosis (Maiuri *et al.*, 1995). The first study showing spontaneous echoes in the arterial system can be attributed to Panidis *et al.* (1984) who reported echogenicity in the aortic arch of patients with aortic dissection. Spontaneous echo contrast in the descending aorta of 8 out of 1014 consecutive patients followed by transesophageal echocardiography was attributed to erythrocyte aggregation (deFilippi *et al.*, 1994). In a retrospective study on 343 patients, 19% showed spontaneous transesophageal echoes in the aorta (Finkelhor *et al.*, 1995). This subgroup of patients was composed of elderly men with slightly larger aortas and complex aortic atherosclerosis. No link between the presence of these echoes and RBC aggregation was made although large vessels and atherosclerosis may be two factors related to enhanced levels of erythrocyte aggregation (Demiroglu *et al.*, 1996; Cloutier *et al.*, 1997). Of 102 consecutive patients suspected of having heart disease, 19% showed transesophageal echoes in the descending aorta (Sukernik *et al.*, 1996). In that study, the spontaneous echoes were velocity-dependent and associated with chronic atrial arrhythmia.

Two recent studies were specifically designed to assess hyper-erythrocyte aggregation *in vivo* in humans (Kitamura and Kawasaki, 1997; Cloutier *et al.*, 1997). Kitamura and Kawasaki (1997) studied the kinetics of rouleau formation in 50 patients suffering from various diseases (mainly cancers). The extent of RBC aggregation was assessed by videodensitometry of B-mode images collected from the subcutaneous vein in the forearm. The echogenicity increase after 2 min of occlusion was obtained by manual compression of the skin using double tourniquets. Following flow stoppage, the echogenicity of blood visibly increased by approximately 18 dB. The echogenicity at 2 min was positively

correlated with the fibrinogen concentration, total cholesterol, and serum protein fraction excluding albumin, and negatively correlated with triglycerides. This study showed that the kinetics of RBC aggregation can be assessed *in vivo* with ultrasound under static conditions. Possible limitations of this study are the absence of recordings during the whole process of rouleau formation, the lack of sensitivity of B-mode imaging to the aggregation of a few RBC before flow stoppage, and the fact that rouleau buildup may not have been completed at 2 min for patients with hyper-erythrocyte aggregation kinetics.

Our group recently assessed differences in the level of RBC aggregation between veins and arteries of normolipidemic and hyperlipidemic individuals (Cloutier *et al.*, 1997). Measurements were performed at the center of several vessels under flowing conditions using power Doppler ultrasound. Because this technique used high-pass filters to remove echoes from high echogenic tissues, its dynamic range is optimized to detect flowing RBC. As a consequence of this, power Doppler ultrasound should be more sensitive than B-mode imaging to small aggregates consisting of a few RBC. Using Doppler ultrasound, stronger backscattered powers were found in veins compared to arteries for recordings in lower limbs. The lower shear rate in veins explains the stronger backscattered power obtained. In comparison to healthy subjects, stronger backscattered powers were also measured in hyperlipidemic individuals for the femoral and popliteal segments. These differences are explained by the enhancement of RBC aggregation in patients. Up to 10 dB power differences were found between the veins of patients and the arteries of healthy subjects. A multiple linear regression analysis was used to assess the relationship between the backscattered power and the diameter of the vessel, maximum blood velocity, lipid profile, blood pressure, body mass index, fibrinogen concentration, and RBC aggregation indices measured with a laser scattering instrument. The parameters explaining the backscattered power variations were an aggregation kinetic index and the diameter of the vessels. This study demonstrated for the first time that power Doppler ultrasound can detect RBC aggregation *in vivo* in human large vessels. Very recently, our group used the power Doppler imaging technology to assess, qualitatively, the differences in RBC aggregation between the superficial femoral artery and the femoral vein of a pregnant woman. As seen in Fig. 7, a stronger backscattered power was found in the femoral vein. This result can be explained by the lower shear rate in the vein and the enhanced level of RBC aggregation in a normal pregnancy (Huisman *et al.*, 1988).

Conclusion

This review has focused on theoretical and computer models of ultrasound backscattering by RBC, on experimental factors affecting the backscattered power from blood, on the use of ultrasound to characterize RBC aggregation, and finally on *in vivo* studies reporting echoes attributable to RBC aggregation and studies aimed at characterizing the importance of RBC aggregation in human vessels. Other reviews can be found in the literature on ultrasound backscattering by RBC (Shung *et al.*, 1993; Shung and Thieme, 1993). However, the current article puts emphasis on the phenomenon of RBC aggregation which is believed to play a significant role in vessel thrombosis and microcirculatory disorders (Stoltz and Donner, 1987).

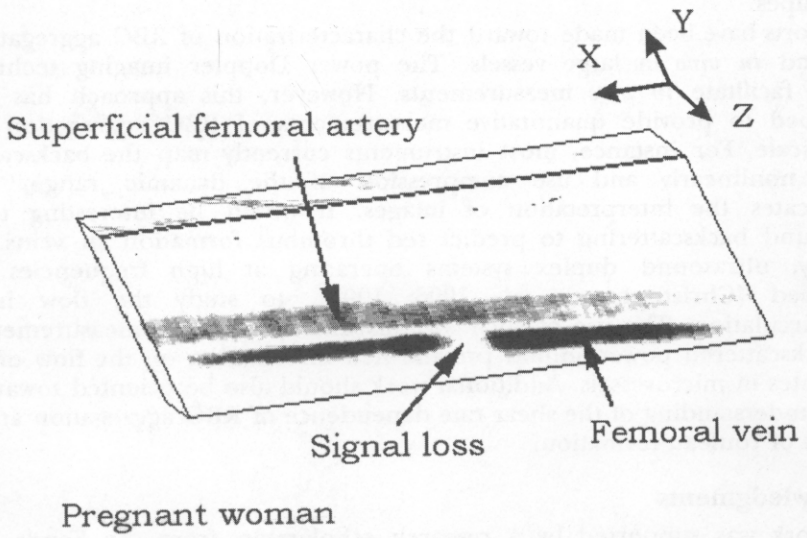

Fig. 7. Example of a longitudinal tridimensional (3-D) power Doppler image of the superficial femoral artery and femoral vein of a normal pregnant woman. A stronger backscattered power is observed over the femoral vein. The signal loss is due to the presence of blood flow velocities below the high-pass wall filter (respiratory artifact). A motor-driven translation assembly allowed the scanning of the ATL linear array probe (L7-4) over the leg. The 3-D imaging instrument was developed by Life Imaging System Inc., (London, Canada). We would like to thank Dr. Helen Routh from ATL (Advanced Technology Laboratories, Seattle, USA) for the use of the Ultramark HDI-9 system equipped with the power Doppler technology that was used to obtain this figure.

Ultrasound backscattering is a very promising technique to study the rheological properties of blood because it can provide a real time, non-invasive, and *in vivo* assessment of RBC aggregation. Ultrasound scattering theories as well as several experimental studies demonstrated that the ultrasound backscattered power is strongly affected by the size of RBC aggregates and rouleau orientation. Ultrasound backscattering was shown to be very sensitive to the shear rate dependence of RBC aggregation and the kinetics of rouleau formation. The study of the mechanisms leading to the "black hole" phenomenon helps us understand some aspects of the rheology of RBC aggregation.

Future developments

It was suggested that ultrasound backscattering may be used to measure the hematocrit and the concentration of fibrinogen *in vivo* (Borders *et al.*, 1978; Shung and Lam, 1991). Considering the complex interrelationship between the numerous factors that affect ultrasound backscattering, this may not be realistic. As a method to characterize blood flow turbulence (Cloutier *et al.*, 1996a), ultrasound backscattering has never been applied *in vivo*. This may be related to the fact that the backscattered power increase under turbulent flow is of the order of 3 to 4 dB, which is much smaller than the power increase attributed to RBC aggregation. Future developments may thus be oriented toward the characterization of RBC aggregation and the development of

theoretical models to predict the scattering by RBC aggregates of different sizes and shapes.

Efforts have been made toward the characterization of RBC aggregation *in vitro* and *in vivo* in large vessels. The power Doppler imaging technology should facilitate *in vivo* measurements. However, this approach has to be developed to provide quantitative measurements of RBC aggregation on a linear scale. For instance, most instruments currently map the backscattered power nonlinearly and use compression of the dynamic range, which complicates the interpretation of images. It would be interesting to use ultrasound backscattering to predict red thrombus formation in veins. Very recently, ultrasound duplex systems operating at high frequencies were developed (Christopher *et al.*, 1996; 1997), to study the flow in the microcirculation. The use of such systems and quantitative measurements of the backscattered power should provide new information on the flow of RBC aggregates in microvessels. Additional work should also be oriented toward the better understanding of the shear rate dependence of RBC aggregation and the kinetics of rouleau formation.

Acknowledgments

This work was supported by a research scholarship from the Fonds de la recherche en santé du Québec, and by grants from the Medical Research Council of Canada (#MT-12491), the Whitaker Foundation, USA, and the Heart and Stroke Foundation of Quebec.

References

ALBRIGHT, R.J., AND HARRIS, J.H. (1975). Diagnosis of urethral flow parameters by ultrasonic backscatter. *IEEE Trans. Biomed. Eng. 22*, 1–11.

ALLARD, L., CLOUTIER, G., AND DURAND, L.G. (1996). Effect of the insonification angle on the Doppler backscattered power under red blood cell aggregation conditions. *IEEE Trans. Ultrason. Ferroelec. Freq. Cont. 43*, 211–219.

ANGELSEN, B.A.J. (1980). A theoretical study of the scattering of ultrasound from blood. *IEEE Trans. Biomed. Eng. 27*, 61–67.

BASCOM, P.A.J., COBBOLD, R.S.C., ROUTH, H.F., AND JOHNSTON, K.W. (1993). On the Doppler signal from a steady flow asymmetrical stenosis model: Effects of turbulence. *Ultrasound Med. Biol. 19*, 197–210.

BASCOM, P.A.J., AND COBBOLD, R.S.C. (1995). On a fractal packing approach for understanding ultrasonic backscattering from blood. *J. Acoust. Soc. Am. 98*, 3040–3049.

BASCOM, P.A.J., JOHNSTON, K.W., COBBOLD, R.S.C., AND OJHA, M. (1997). Relation of the flow field distal to a moderate stenosis to the Doppler power. *Ultrasound Med. Biol. 23*, 25–39.

BEPPU, S., NIMURA, Y., SAKAKIBARA, H., NAGATA, S., PARK, Y.D., IZUMI, S., UEOKA, M., MASUDA, Y., AND NAKASONE, I. (1985). Smoke-like echo in the left atrial cavity in mitral valve disease: Its features and significance. *J. Am. Coll. Cardiol. 6*, 744–749.

BERGER, N.E., LUCAS, R.J., AND TWERSKY, V. (1991). Polydisperse scattering theory and comparisons with data for red blood cells. *J. Acoust. Soc. Am. 89,* 1394–1401.

BLACK, I.W., HOPKINS, A.P., LEE, L.C.L., WALSH, W.F., AND JACOBSON, B.M. (1991). Left atrial spontaneous echo contrast: A clinical and echocardiographic analysis. *J. Am. Coll. Cardiol. 18,* 398–404.

BORDERS, S.E., FRONEK, A., KEMPER, W.S., AND FRANKLIN, D. (1978). Ultrasonic energy backscattered from blood: An experimental determination of the variation of sound energy with hematocrit. *Ann. Biomed. Eng. 6,* 83–92.

BOYNARD, M., LELIEVRE, J.C., AND GUILLET, R. (1987). Aggregation of red blood cells studied by ultrasound backscattering. *Biorheology 24,* 451–461.

BOYNARD, M., AND LELIEVRE, J.C. (1990). Size determination of red blood cell aggregates induced by dextran using ultrasound backscattering phenomenon. *Biorheology 27,* 39–46.

BOYNARD, M., MILLS, P., HAMMI, E., AND GUILLET, R. (1994). Formation d'agrégats de globules rouges dans un écoulement de sédimentation mesuré par rétrodiffusion ultrasonore et modélisation des cinétiques d'agrégation. *Innov. Tech. Biol. Med. 15,* 215–228.

BRILEY, D.P., GIRAUD, G.D., BEAMER, N.B., SPEAR, E.M., GRAUER, S.E., EDWARDS, J.M., CLARK, W.M., SEXTON, G.J., AND COULL, B.M. (1994). Spontaneous echo contrast and hemorheologic abnormalities in cerebrovascular disease. *Stroke 25,* 1564–1569.

BRODY, W.R., AND MEINDL, J.D. (1974). Theoretical analysis of the CW Doppler ultrasonic flowmeter. *IEEE Trans. Biomed. Eng. 21,* 183–192.

CHIEN, S. (1976). Electrochemical interactions between erythrocyte surfaces. *Thromb. Res. 8,* 189–202.

CHRISTOPHER, D.A., BURNS, P.N., ARMSTRONG, J., AND FOSTER, F.S. (1996). A high-frequency continuous-wave Doppler ultrasound system for the detection of blood flow in the microcirculation. *Ultrasound Med. Biol. 22,* 1191–1203.

CHRISTOPHER, D.A., BURNS, P.N., STARKOSKI, B.G., AND FOSTER, F.S. (1997). A high-frequency pulsed-wave Doppler ultrasound system for the detection and imaging of blood flow in the microcirculation. *Ultrasound Med. Biol. 23,* 997–1015.

CLOUTIER, G., AND SHUNG, K.K. (1991). Cyclic variation of Doppler backscattering power from porcine blood in a pulsatile flow model. *IEEE Ultrasonics Symposium 2,* 1301–1304.

CLOUTIER, G., AND SHUNG, K.K. (1993a). Cyclic variation of the power of ultrasonic Doppler signals backscattered by polystyrene microspheres and porcine erythrocyte suspensions. *IEEE Trans. Biomed. Eng. 40,* 953–962.

CLOUTIER, G., AND SHUNG, K.K. (1993b). Study of red cell aggregation in pulsatile flow from ultrasonic Doppler power measurements. *Biorheology 30*, 443–461.

CLOUTIER, G., ALLARD, L., AND DURAND, L.G. (1995). Changes in ultrasonic Doppler backscattered power downstream of concentric and eccentric stenoses under pulsatile flow. *Ultrasound Med. Biol. 21*, 59–70.

CLOUTIER, G., ALLARD, L., AND DURAND, L.G. (1996a). Characterization of blood flow turbulence with pulsed-wave and power Doppler ultrasound imaging. *J. Biomech. Eng. 118*, 318–325.

CLOUTIER, G., QIN, Z., DURAND, L.G., AND TEH, B.G. (1996b). Power Doppler ultrasound evaluation of the shear rate and shear stress dependences of red blood cell aggregation. *IEEE Trans. Biomed. Eng. 43*, 441–450.

CLOUTIER G., AND QIN Z. (1997). Shear rate dependence of normal, hypo-, and hyper-aggregating erythrocytes studied with power Doppler ultrasound. In: *Acoustical Imaging*. 23. S. Lees and L.A. Ferrari, Eds., Plenum Publishing Corporation, New York, pp. 291–296.

CLOUTIER, G., WENG, X., ROEDERER, G.O., ALLARD, L., TARDIF, F., AND BEAULIEU, R. (1997). Differences in the erythrocyte aggregation level between veins and arteries of normolipidemic and hyperlipidemic individuals. *Ultrasound Med. Biol. 23*, 1383–1393.

COBET, U. (1988). Modelling of ultrasound scattering by blood. *J. Nucl. Med. Allied Sciences 32*, 188–195.

COPLEY A.L., KING R.G., AND HUANG, C.R. (1976). Erythrocyte sedimentation of human blood at varying shear rates. In: *Microcirculation*. 1, J. Grayson and W. Zingg, Eds., Plenum Press, New York, pp. 133–134.

DANIEL, W.G., NELLESSEN, U., SCHRÖDER, E., NONNAST-DANIEL, B., BEDNARSKI, P., NIKUTTA, P., AND LICHTLEN, P.R. (1988). Left atrial spontaneous echo contrast in mitral valve disease: An indicator for an increased thromboembolic risk. *J. Am. Coll. Cardiol. 11*, 1204–1211.

DEFILIPPI, C.R., LACKER, M., GRAYBURN, P.A., AND BRICKNER, M.E. (1994). Spontaneous echo contrast in the descending aorta detected by transesophageal echocardiography. *Am. J. Cardiol. 74*, 410–411.

DE KROON, M.G.M., SLAGER, C.J., GUSSENHOVEN, W.J., SERRUYS, P.W., ROELANDT, J.R.T.C., AND BOM, N. (1991). Cyclic changes of blood echogenicity in high-frequency ultrasound. *Ultrasound Med. Biol. 17*, 723–728.

DEMIROGLU, H., BARISTA, I., AND DÜNDAR, S. (1996). Erythrocyte aggregability in patients with coronary heart disease. *Clin. Hemorheol. 16*, 313–317.

ERBEL, R., STERN, H., EHRENTHAL, W., SCHREINER, G., TREESE, N., KRÄMER, G., THELEN, M., SCHWEIZER, P., AND MEYER, J. (1986). Detection of spontaneous echocardiographic contrast within the left atrium by transesophageal echocardiography: Spontaneous echocardiographic contrast. *Clin. Cardiol. 9,* 245–252.

EVANS, D.H., MCDICKEN, W.N., SKIDMORE, R., AND WOODCOCK, J.P. (1989). *Doppler Ultrasound Physics, Instrumentation, and Clinical Applications.* 1st edition. D.H. Evans, W.N. McDicken, R. Skidmore, and J.P. Woodcock, Eds., John Wiley & Sons, Chichester, New York, Brisbane, Toronto, Singapore, 287 pp.

FATKIN, D., LOUPAS, T., LOW, J., AND FENELEY, M. (1997). Inhibition of red cell aggregation prevents spontaneous echocardiographic contrast formation in human blood. *Circulation 96,* 889–896.

FINKELHOR, R.S., LAMONT, W.E., RAMANAVARAPU, S.K., AND BAHLER, R.C. (1995). Spontaneous echocardiographic contrast in the thoracic aorta: Factors associated with its occurrence and its association with embolic events. *Am. Heart J. 130,* 1254–1258.

GOUGH, W., ROUTH, H.F., AND WILLIAMS, R.P. (1988). Weak reflection of a wave by a one-dimensional array of randomly spaced elements, with reference to the scattering of ultrasound by blood. *Phys. Med. Biol. 33,* 793–804.

HANSS, M., AND BOYNARD, M. (1979). Ultrasound backscattering from blood: Hematocrit and erythrocyte aggregation dependence. In: *Ultrasonic Tissue Characterization II.* M. Linzer, Ed., pp. 165–169.

HJEMDAHL-MONSEN, C.E., DANIELS, J., KAUFMAN, D., STERN, E.H., TEICHHOLZ, L.E., AND MELTZER, R.S. (1984). Spontaneous contrast in the inferior vena cava in a patient with constrictive pericarditis. *J. Am. Coll. Cardiol. 4,* 165–167.

HUISMAN, A., AARNOUDSE, J.G., KRANS, M., HUISJES, H.J., FIDLER, V., AND ZIJLSTRA, W.G. (1988). Red cell aggregation during normal pregnancy. *Br. J. Haematol. 68,* 121–124.

HUNT, J.W., WORTHINGTON, A.E., AND KERR, A.T. (1995). The subtleties of ultrasound images of an ensemble of cells: Simulation from regular and more random distributions of scatterers. *Ultrasound Med. Biol. 21,* 329–341.

HWANG, J.J., KUAN, P., CHEN, J.J., KO, Y.L., CHENG, J.J., LIN, J.L., TSENG, Y.Z., AND LIEN, W.P. (1994). Significance of left atrial spontaneous echo contrast in rheumatic mitral valve disease as a predictor of systemic arterial embolization: A transesophageal echocardiographic study. *Am. Heart J. 127,* 880–885.

KEARNEY, K., AND MAHONY, C. (1995). Effect of aspirin on spontaneous contrast in the brachial veins of normal subjects. *Am. J. Cardiol. 75,* 924–928.

KIM, S.Y., MILLER, I.F., SIGEL, B., CONSIGNY, P.M., AND JUSTIN, J. (1989). Ultrasonic evaluation of erythrocyte aggregation dynamics. *Biorheology 26,* 723–736.

KITAMURA, H., SIGEL, B., MACHI, J., FELEPPA, E.J., SOKIL-MELGAR, J., KALISZ, A., AND JUSTIN, J. (1995). Roles of hematocrit and fibrinogen in red cell aggregation determined by ultrasonic scattering properties. *Ultrasound Med. Biol. 21,* 827–832.

KITAMURA, H., AND KAWASAKI, S. (1997). Detection and clinical significance of red cell aggregation in the human subcutaneous vein using a high-frequency transducer (10 MHz): A preliminary report. *Ultrasound Med. Biol. 23,* 933–938.

KUO, I.Y., AND SHUNG, K.K. (1994). High frequency ultrasonic backscatter from erythrocyte suspension. *IEEE Trans. Biomed. Eng. 41,* 29–34.

LIM, B., BASCOM, P.A.J., AND COBBOLD, R.S.C. (1996). Particle and voxel approaches for simulating ultrasound backscattering from tissue. *Ultrasound Med. Biol. 22,* 1237–1247.

LUCAS, R.J., AND TWERSKY, V. (1987). Inversion of ultrasonic scattering data for red blood cell suspensions under different flow conditions. *J. Acoust. Soc. Am. 82,* 794–799.

MACHI, J., SIGEL, B., BEITLER, J.C., COELHO, J.C.U., AND JUSTIN, J.R. (1983). Relation of in vivo blood flow to ultrasound echogenicity. *J. Clin. Ultrasound 11,* 3–10.

MACHI, J., SIGEL, B., RAMOS, J.R., JUSTIN, J.R., FEINBERG, H., LEBRETON, G.C., AND ROBERTSON, A.L., Jr. (1984). Ultrasonic detection of platelet aggregation at variable shear rates. *Haemostasis 14,* 473–479.

MACHI, J., SIGEL, B., AND FEINBERG, H. (1987). Protamine-induced platelet aggregation and clotting investigated by ultrasound. *Haemostasis 17,* 226–234.

MAHONY, C. (1987). The ultrasonic detection of platelet aggregates. *Thromb. Res. 47,* 665–672.

MAHONY, C., SUBLETT, K.L., AND HARRISON, M.R. (1989). Resolution of spontaneous contrast with platelet disaggregatory therapy (Trifluoperazine). *Am. J. Cardiol. 63,* 1009–1010.

MAHONY, C., SPAIN, C., SPAIN, M., EVANS, J., FERGUSON, J., AND SMITH, M.D. (1994). Intravascular platelet aggregation and spontaneous contrast. *J. Ultrasound Med. 13,* 443–450.

MAIURI, F., GALLICCHIO, B., IACONETTA, G., BERNARDO, A., AND SERRA, L.L. (1995). Ultrasonographic findings that predict carotid restenosis after endoarterectomy. *Eur. J. Ultrasound 2,* 261–267.

MO, L.Y.L., AND COBBOLD, R.S.C. (1986). A stochastic model of the backscattered Doppler ultrasound from blood. *IEEE Trans. Biomed. Eng. 33,* 20–27.

MO, L.Y.L., YIP, G., COBBOLD, R.S.C., GUTT, C., JOY, M., SANTYR, G., AND SHUNG, K.K. (1991). Non-newtonian behavior of whole blood in a large diameter tube. *Biorheology 28*, 421–427.

MO, L.Y.L., AND COBBOLD, R.S.C. (1992). A unified approach to modeling the backscattered Doppler ultrasound from blood. *IEEE Trans. Biomed. Eng. 39*, 450–461.

MO, L.Y.L., KUO, I.Y., SHUNG, K.K., CERESNE, L., AND COBBOLD, R.S.C. (1994). Ultrasound scattering from blood with hematocrits up to 100%. *IEEE Trans. Biomed. Eng. 41*, 91–95.

PANIDIS, I.P., KOTLER, M.N., MINTZ, G.S., AND ROSS, J. (1984). Intracavitary echoes in the aortic arch in type III aortic dissection. *Am. J. Cardiol. 54*, 1159–1160.

QIN, Z., DURAND, L.G., AND CLOUTIER, G. (1998a). Kinetics of the "black hole" phenomenon in ultrasound backscattering measurements with red blood cell aggregation. *Ultrasound Med. Biol. 24*, 245–256.

QIN, Z., DURAND, L.G., ALLARD, L., AND CLOUTIER, G. (1998b). Effects of a sudden flow reduction on red blood cell rouleau formation and orientation using RF backscattered power. *Ultrasound Med. Biol. 24*, (in press).

RAYLEIGH J.W.S. (1945). Vibrations of solid bodies. In: *Theory of sound.* 2, Dover Publications, New York, pp. 414–431.

RAZAVIAN, S.M., LEVENSON, J., PERONNEAU, P., AND SIMON, A. (1995). Quantification of erythrocyte aggregation by blood echogenicity: a preliminary study. *J. Cardiovasc. Surg. 36*, 375–377.

ROUTH, H.F., GOUGH, W., AND WILLIAMS, R.P. (1987). One-dimensional computer simulation of a wave incident on randomly distributed inhomogeneities with reference to the scattering of ultrasound by blood. *Med. Biol. Eng. Comput. 25*, 667–671.

ROUTH, H.F., WILLIAMS, R.P., AND GOUGH, W. (1989). Weak reflection of ultrasound by elements arranged in the steps of a one-dimensional random walk, with reference to backscatter by blood. *Med. Biol. Eng. Comput. 27*, 198–203.

SCHUCHMAN, H., FEIGENBAUM, H., DILLON, J.C., AND CHANG, S. (1975). Intracavitary echoes in patients with mitral prosthetic valves. *J. Clin. Ultrasound 3*, 107–110.

SENNAOUI, A., BOYNARD, M., AND PAUTOU, C. (1997). Characterization of red blood cell aggregate formation using an analytical model of the ultrasonic backscattering coefficient. *IEEE Trans. Biomed. Eng. 44*, 585–591.

SHEHADA, R.E.N., COBBOLD, R.S.C., AND MO, L.Y.L. (1994). Aggregation effects in whole blood: Influence of time and shear rate measured using ultrasound. *Biorheology 31*, 115–135.

SHEN, W.F., TRIBOUILLOY, C., RIDA, Z., PELTIER, M., CHOQUET, D., REY, J.L., AND LESBRE, J.P. (1996). Clinical significance of intracavitary spontaneous echo contrast in patients with dilated cardiomyopathy. *Cardiology 87,* 141–146.

SHUNG, K.K., SIGELMANN, R.A., AND REID, J.M. (1976). Scattering of ultrasound by blood. *IEEE Trans. Biomed. Eng. 23,* 460–467.

SHUNG, K.K., SIGELMANN, R.A., AND REID, J.M. (1977). Angular dependence of scattering of ultrasound from blood. *IEEE Trans. Biomed. Eng. 24,* 325–331.

SHUNG, K.K., AND REID, J.M. (1979). Ultrasonic instrumentation for hematology. *Ultrasonic Imaging 1,* 280–294.

SHUNG, K.K. (1982). On the ultrasound scattering from blood as a function of hematocrit. *IEEE Trans. Sonics. Ultra 29,* 327–331.

SHUNG, K.K., YUAN, Y.W., FEI, D.Y., AND TARBELL, J.M. (1984). Effect of flow disturbance on ultrasonic backscatter from blood. *J. Acoust. Soc. Am. 75,* 1265–1272.

SHUNG, K.K., AND LAM, P. (1991). An ultrasonic method for assaying blood fibrinogen. *Ann. Inter. Conf. IEEE Eng. Med. Biol. Soc. 13,* 156–157.

SHUNG, K.K., CLOUTIER, G., AND LIM, C.C. (1992). The effects of hematocrit, shear rate, and turbulence on ultrasonic Doppler spectrum from blood. *IEEE Trans. Biomed. Eng. 39,* 462–469.

SHUNG, K.K., KUO, I.Y., AND CLOUTIER G. (1993). Ultrasonic scattering properties of blood. In: *Intravascular Ultrasound.* J. Roelandt, E.J. Gussenhoven and N. Bom, Eds., Kluwer Academic Publishers, Dordrechet, Holland, pp. 119–139.

SHUNG, K.K., AND THIEME, G.A. (1993). *Ultrasonic scattering in biological tissues.* 1st edition. K.K. Shung and G.A. Thieme, Eds., CRC Press, Boca Raton, Ann Arbor, London, Tokyo, 486 pp.

SHUNG, K.K., AND KUO, I.Y. (1994). Analysis of ultrasonic scattering in blood via a continuum approach. *Ultrasound Med. Biol. 20,* 623–627.

SIGEL, B., MACHI, J., BEITLER, J.C., JUSTIN, J.R., AND COELHO, J.C.U. (1982). Variable ultrasound echogenicity in flowing blood. *Science 218,* 1321–1323.

SIGEL, B., MACHI, J., BEITLER, J.C., AND JUSTIN, J.R. (1983). Red cell aggregation as a cause of blood-flow echogenicity. *Radiology 148,* 799–802.

SIOSTRZONEK, P., KOPPENSTEINER, R., GÖSSINGER, H., ZANGENEH, M., HEINZ, G., KREINER, G., STÜMPFLEN, A., BUXBAUM, P., EHRINGER, H., AND MÖSSLACHER, H. (1993). Hemodynamic and hemorheologic determinants of left atrial

spontaneous echo contrast and thrombus formation in patients with idiopathic dilated cardiomyopathy. *Am. Heart J. 125,* 430–434.

STOLTZ, J.F., AND DONNER, M. (1987). Hemorheology: Importance of erythrocyte aggregation. *Clin. Hemorheol. 7,* 15–23.

STOLTZ, J.F., AND DONNER, M. (1991). Red blood cell aggregation: Measurements and clinical applications. *Tr. J. of Medical Sciences 15,* 26–39.

SUKERNIK, M.R., WEST, O., LAWAL, O., CHITTIVELU, B., HENDERSON, R., SHERZOY, A.A., VANDERBUSH, E.J., AND FRANCIS, C.K. (1996). Hemodynamic correlates of spontaneous echo contrast in the descending aorta. *Am. J. Cardiol. 77,* 184–186.

TWERSKY, V. (1987). Low-frequency scattering by correlated distributions of randomly oriented particles. *J. Acoust. Soc. Am. 81,* 1609–1618.

TWERSKY, V. (1988). Low-frequency scattering by mixtures of correlated nonspherical particles. *J. Acoust. Soc. Am. 84,* 409–415.

VAN DER HEIDEN, M.S., DE KROON, M.G.M., BOM, N., AND BORST, C. (1995). Ultrasound backscatter at 30 MHz from human blood: influence of rouleau size affected by blood modification and shear rate. *Ultrasound Med. Biol. 21,* 817–826.

WANG, X.F., LIU, L., CHENG, T.O., LI, Z.A., DENG, Y.B., AND WANG, J.E. (1992). The relationship between intracardiovascular smoke-like echo and erythrocyte rouleaux formation. *Am. Heart J. 124,* 961–965.

WENG, X., CLOUTIER, G., PIBAROT, P., AND DURAND, L.G. (1996). Comparison and simulation of different levels of erythrocyte aggregation with pig, horse, sheep, calf, and normal human blood. *Biorheology 33,* 365–377.

WU, S.J., AND SHUNG, K.K. (1996). Cyclic variation of Doppler power from whole blood under pulsatile flow. *Ultrasound Med. Biol. 22,* 883–894.

YAMADA, E.G., FITZGERALD, P.J., SUDHIR, K., HARGRAVE, V.K., AND YOCK, P.G. (1992). Intravascular ultrasound imaging of blood: The effect of hematocrit and flow on backscatter. *J. Am. Soc. Echocardiogr. 5,* 385–392.

YUAN, Y.W., AND SHUNG, K.K. (1988a). Ultrasonic backscatter from flowing whole blood: I. Dependence on shear rate and hematocrit. *J. Acoust. Soc. Am. 84,* 52–58.

YUAN, Y.W., AND SHUNG, K.K. (1988b). Ultrasonic backscatter from flowing whole blood: II. Dependence on frequency and fibrinogen concentration. *J. Acoust. Soc. Am. 84,* 1195–1200.

YUAN, Y.W., AND SHUNG, K.K. (1989). Echoicity of whole blood. *J. Ultrasound Med. 8,* 425–434.

ZHANG, J., ROSE, J.L., AND SHUNG, K.K. (1994). A computer model for simulating ultrasonic scattering in biological tissues with high scatterer concentration. *Ultrasound Med. Biol. 20,* 903–913.

Received 30 October 1997; accepted in revised form 4 February 1998.